# Anti-fall-attract Control of Permanent Magnetism Suspension System with Flux Path Control

Jinghu Tang[1] ,Qiang Li[1],Feng Sun[1],Chuan Zhao[1],Junjie Jin[1],Yongquan Guo[1], Fangchao Xu[1]

[1]Shenyang University of Technology, No.111, Shenliao West Road, Economic and Technological Development Area, Shenyang, China, 15909832169@163.com

**[1]Shenyang University of Technology, Shenyang, China, sunfeng@sut.edu.cn**

**Abstract:** Permanent magnetic levitation is a typical nonlinear system. With the air gap between magnetic conductors and suspensions object is changed, the control characteristics changes and affects the stability of the system. In order to prevent the external interference causing the suspended object falls or attract on it,as the system deviating from the equilibrium point. Anti-fall-Attract Control method based on air gap variation is proposed. According to the selection of multiple design points in the whole air gap, a gain regulation is designed at each design point. Finally, a complete anti-fall and anti-attract control law is obtained by interpolating between these linear controllers,which improves the controllability,stability and robustness of the system. The simulation and experimental results show that the anti-fall and anti-attract control method can effectively compensate for the uneven variation of suspension force when the suspension is moving. External disturbance causes the air gap large, suspension force is increased rapidly, the suspension object can be prevented from falling;External disturbance causes the air gap smaller, suspension force is reduced quickly, the suspension object can be prevented attract to magnetic conductors.

**Key words:** Anti-fall and Anti-attract; variable Magnetic Circuit; permanent Maglev; nonlinear compensation

## Introduction

Magnetic levitation technology use magnetic force to make the object along the axis of linear motion or rotational motion under the attraction or repulsive force. Since it has no contact with the braced frame, energy consumption and speed constraints caused by friction can be avoided,so It has the advantages of long life, no friction, no lubrication and other advantages. Magnetic levitation technology is widely used in spaceflight, bearing and medical field[1-3]. In recent years,with the improvement of the properties of permanent magnetic materials and the appearance of rare earth materials, new permanent magnetic materials have high energy product ratio, no heat,and compact structure is studied by many scholars [4-6].

Beacuse the permanent magnetic levitation system is unstable, it makes the levitation control technology of the system become one of the core technology in this system.The common method of maglev control is to linearize the nonlinear system at the equilibrium point. Based on the linearized model,using an easily implemented feedback control algorithm[7, 8]. When the system deviates from the operating point, the tracking performance of the system becomes worse, fluctuation or even falling down or attract onto the Magnetic conductor ,the system is destroyed. In document[9], a set of anti-suction and death prevention system is designed, which is composed of prediction module and protection module,the gap is detected by the position sensor and the current is shifted by the switch.In document[10,11]by nonlinear combination of position feedback and current feedback, the suspension force increases rapidly when the system deviates from the equilibrium point.

when the system is stable ,the disturbance of the external force is reflected by the variation of the suspending air gap. In this paper,the controllable suspension force is preset at each air gap point,which is further away from the equilibrium position, the force will be greater.

## 1 System structure and working principle

### 1.1 System structure

As shown in figure 1, this is a controllable magnetic circuit permanent magnetic levitation system,which consisting of a DC servo motor, a radial magnetized disk permanent magnet, and a "F" type guide magnet yoke. In the system, the suspended matter are placed directly below the magnetic conductors, and the disk permanent magnets are rotated by the servo motor, which changes the effective magnetic flux through the suspensions, and then controls the magnitude of the levitation force. When the gravity and force of suspension are equal, the stable suspension can be realized.

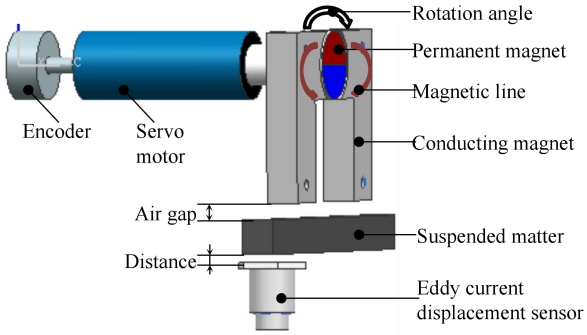


Fig. 1 Structure of permanent magnetism suspension system.

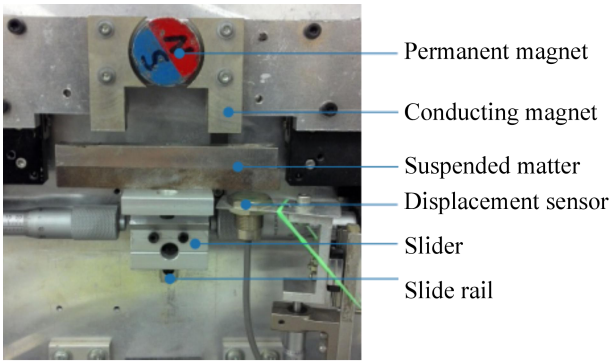


Fig. 2 Permanent magnetic suspension system

## 1.2 Operational principle

For a single working fulcrum, its working principle can be illustrated in Fig. 3 (a) ,when the rotation angle $\theta$ of the disk permanent magnet is 0 °, the magnetic inductance line starts from the *N* pole of the disc permanent magnet and returns to the *S* pole through the magnetic conductor .No magnetic lines passing through suspended object. When the rotation angle $\theta$ of the permanent magnet is greater than 0 °and less than 90 °(Fig. 3 b), a part of the magnetic inductance line starts from the *N* pole and passes through the left magnetic conductor, the suspended object, and the right magnetic conductor back to the *S* pole. A magnetic force is produced between a magnetic conductor and a suspended object, and this part of the magnetic circuit is called the effective magnetic circuit of the system. With the increase of the rotation angle of the disk permanent magnet, the magnetic flux through the suspended matter will also increase, and the magnetic force between the magnetic conductors and the suspended object will also increase. When the magnetic force is equal to the weight of the suspension, the system is stable. By adjusting the angle of the permanent magnet to change the magnetic flux in the effective magnetic circuit, to achieve the purpose of adjusting the magnetic force between the magnetic conductors and the suspension object.

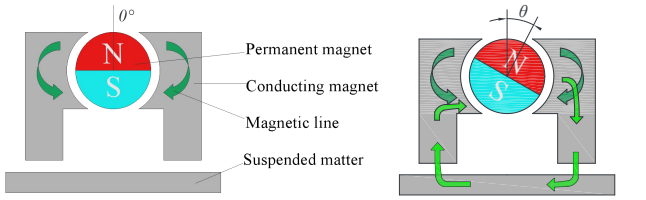


(a)Initial state (b) Magnet rotation angle $\theta$°

Fig. 3 Permanent magnetic levitation principle

# 2 Mathematical modeling

System model diagrams and symbolic definitions are shown in Fig.2,In the figure, $f_m$ is the magnet attraction to the suspension； $d$ is the between the suspension object and the magnetic conductor ;$d_0$ is the distance between the suspension and the magnetic conductor at equilibrium; $z$ is the small displacement of the suspended material in the vertical direction when it deviates from the equilibrium position. $z=d_0-d$ Positive direction upward;$\theta$ is the rotation angle in the clockwise direction of the disk-shaped permanent magnet;$\theta_0$ is the rotation angle of the permanent magnet in the equilibrium state,Deviation from equilibrium position $\Delta\theta=\theta_0-\theta$;$D$ indicates the distance between the disk-shaped permanent magnet and the magnetizer.

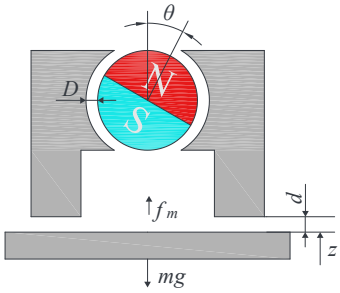


Fig. 4 Model diagram and symbol definition

$K_\tau$ is the torque coefficient of Disc permanent Magnet,$\Delta d_\tau$ is the magnetic flux leakage compensation coefficient at the air gap between disk permanent magnets and magnetic conductors.

According to formula (1) and formula( 2), the expression of kinematics equation of the system can be obtained as follows:

$$J\ddot{\theta} = -c_1\dot{\theta} + k_\tau \frac{\sin 2(\theta_0 - \Delta\theta)}{d_0 - z + \Delta d_\tau} + k_t i \qquad (2)$$

$$m\ddot{z} = -c_2\dot{z} + k_m \frac{\sin^2(\theta_0 - \Delta\theta)}{(d_0 - z + \Delta d_f)^2} - mg - f_d \qquad (3)$$

$J$ is the moment of inertia of the motor and disk magnet, $k_t$ is the servo motor torque factor,$i$ is the servo motor input current,$m$ is the mass of the suspended material,$c_1$ is the damping coefficient of the disc permanent magnet in the direction of rotation.$c_2$ is the damping coefficient of

the suspended solid in the vertical movement direction.$f_d$ is external interference.

At the equilibrium position $z$=0,$\Delta\theta$=0,$f_d$=0 Tylor expansion,Removal of second order minimum：

$$J\Delta\ddot{\theta} = -c_1\Delta\dot{\theta} + a_{41}z + a_{43}\Delta\theta + k_t\Delta i \quad (4)$$

$$m\ddot{z} = -c_2\dot{z} + k_x z + k_\theta\Delta\theta - f_d \quad (5)$$

$$a_{41} = \frac{k_\tau \sin 2\theta_0}{(d_0+\Delta d_\tau)^2} \qquad a_{43} = \frac{2k_\tau \cos 2\theta_0}{(d_0+\Delta d_\tau)}$$

$$k_x = \frac{2k_m(\sin\theta_0)^2}{(d_0+\Delta d_f)^3} \qquad k_\theta = \frac{k_m \sin 2\theta_0}{(d_0+\Delta d_f)^2}$$

The system parameters are shown in Table 1:

Tab.1 Parameters of System

| Parameter | Value |
|---|---|
| Suspended object quality $m$/(kg) | 0.262 |
| Torque magnetic leakage compensation coefficient $\triangle d_\tau$/(mm) | 14 |
| Levitation force magnetic leakage compensation coefficient $\triangle d_f$/(mm) | 1.6 |
| Rotational damping $c_1$/(N/(m/s)) | 0.5 |
| Linear damping $c_2$/(N/(m/s)) | 100 |
| Moment of inertia $J$/(kg·m$^2$) | 6.37×10$^{-4}$ |
| Motor current coefficient $k_t$/ (Nm/A) | 0.69 |
| Levitation force coefficient $k_m$/(Nm$^2$) | 2.45×10$^{-4}$ |
| Torque factor $k_\tau$/(Nm$^2$) | -8.726×10$^{-3}$ |

The controlled object model block diagram:

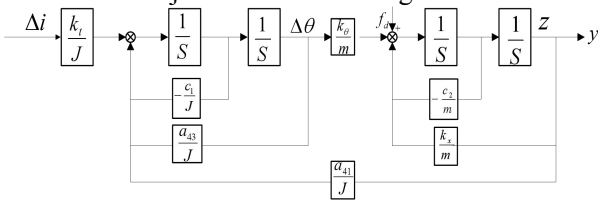


Fig.5 Controlled object model block diagram

# 3 Design of anti-fall and anti-attract controller

In order to facilitate the analysis of the controlled object into two parts,One part is the process of current Δi to angle Δθ, and the other part is the process of angle $\Delta\theta$ to air gap z.It can be seen from the figure that there is positive feedback $a41/J$ in the controlled object,The angle Δθ is not only affected by the current $\Delta i$, but also affected by z,which increases the difficulty of the analysis.However, the change of z actually has little effect on Δθ. The equivalent substitution of the graph is performed, and the equivalent model of Fig. 6 is obtained.

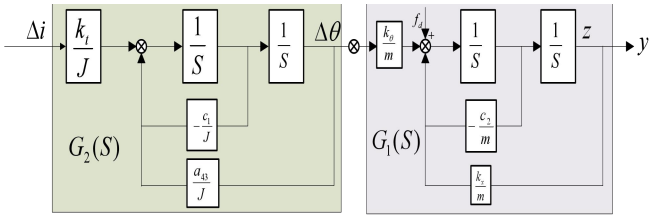


Fig.6 Controlled object model block diagram equivalent

$$G_1(S) = \frac{\Delta\theta}{\Delta i} = \frac{k_t}{JS^2 + c_1 S - a_{43}} \quad (7)$$

$$G_2(S) = \frac{z}{\Delta\theta} = \frac{k_\theta}{mS^2 + c_2 S - k_x} \quad (8)$$

## 3.1 Analysis of control characteristics analysis

As shown in Fig 8, double closed-loop control of the current loop and position loop.

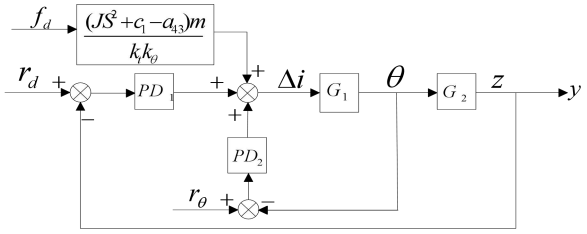


Fig.7 Double closed loop parallel control block diagram

The control amount u(t) is shown as follows:

$$u(t) = K_{p_1}[e_1(t) + T_{d1}\frac{de_1(t)}{dt}] + K_{p_2}[e_2(t) + T_{d2}\frac{de_2(t)}{dt}] \quad (9)$$
$$= Kp_1 z + Kd_1\dot{z} + Kp_2\Delta\theta + Kd_2\Delta\dot{\theta}$$

When there is an external disturbance input, the control amount changes, and the current is adjusted by the current loop and the position loop to stabilize the system.

Two conditions need to be satisfied for the stability of the system:

$$① F = k_m\frac{\sin^2\theta}{(d+\Delta d_f)^2} = mg + f_d \quad (10)$$

$$② \Delta i = K_{p1}\Delta d + K_{d1}\Delta\dot{d} + K_{p2}\Delta\theta + K_{d2}\Delta\dot{\theta} = 0 \quad (11)$$

From the above formula can be derived $\frac{K_{p1}}{K_{p2}} = \frac{\Delta\theta}{\Delta d}$ (12)

$K_{p1}$ and $K_{p2}$ are air gap error gain and angle error gain respectively,These parameters do not change with the system after setting, so $\Delta\theta$ and $\Delta d$ are proportional relationships, and one micro-displacement $\Delta d$ corresponds to one $\Delta\theta$.

Setting $K_{p1}/K_{p2} = \frac{\Delta\theta}{\Delta d} = k_j$ （$j$ =1,2,3,4,5），

Set the balance point to ($d_0$=5mm,$\theta_0$=43°)Air gap range $d$=2.5~6.5$mm$. As shown in Fig 9, the relationship between the angle deviation and air gap deviation. Fig 10, the actual air gap and angle relationship.

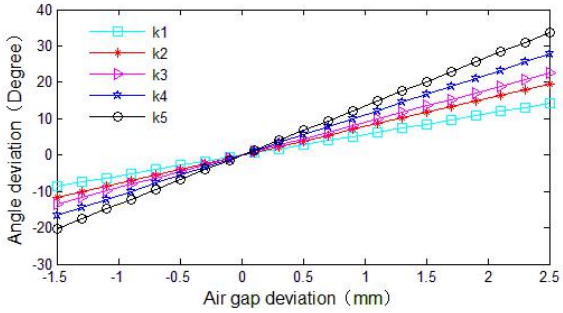

Fig.8 Relationship between angular deviation and air gap deviation

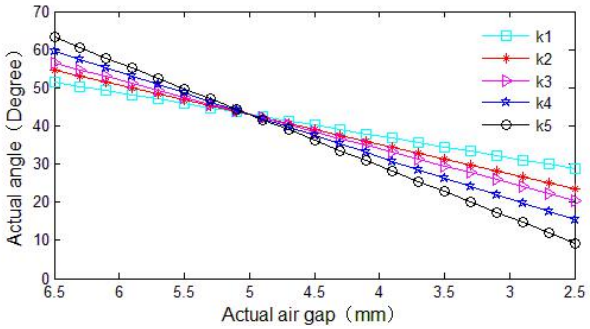

Fig.9 Relationship between actual air gap and actual angle

From Fig.4, we can see that regardless of the value of $k_j$, the air gap and the angle change linearly.Therefore, as long as the value of $k_j$ is determined, the angle of the permanent magnet and the air gap of the suspension are also uniquely determined.In the range of air gap, with the increase of $k_j$ value, the range of angle change also increases.

Combining the data in Table 1, the variation of the levitation force with the air gap at different $k_j$ is obtained as shown in Fig.11.

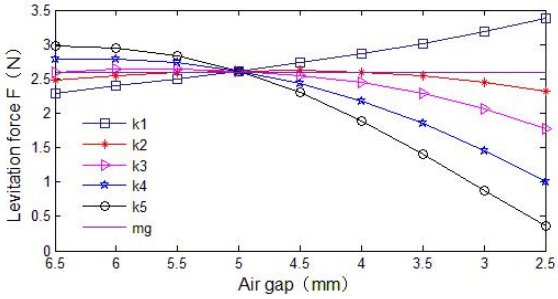

Fig.10 The relationship between the variation of suspension force with air gap and the gravity of suspended substance

It can be seen from the figure that as the air gap decreases, the difference between the levitation force $F$ and the gravity $mg$ increases.The small difference on the left side of the equilibrium point causes the system's levitation force to be insufficient, and the large difference on the right side of the equilibrium point causes system oscillation. If ensure that there is enough levitation force on the left side, it will cause excessive overshoot on the right side, and If the right side is stabilized, the levitation force of the left side will be insufficient.

From the above analysis, it can be concluded that the air gap $d$ and the angle $\theta$ are linear under the control of the gains $K_{p1}$ and $K_{p2}$. However, the suspension force F and the suspended object gravity $mg$ have a nonlinear relationship under the control of the gains $K_{p1}$ and $K_{p2}$. When there is external disturbance, there will be oscillations, and even suspended matter will fall and attract on the magnetic conductor.

## 3.2 Design of anti-fall and anti-attract controller

In the case of oscillation, fall and attract of suspended solids,this article proposes the anti-fall and anti-attract control of suspended object. Anti-fall-attract controller, first according to the air gap preset suspension force $F$, and then design the control parameter $Kp$ according to the levitation force $F$.Considering the impact of the load on the system, when the external load $f_d$ is added, the following equation is obtained:

$$F = mg + f_d = k_m \frac{\sin^2(\theta_0 + \Delta\theta)}{(d_0 + \Delta d + \Delta d_f)^2} \tag{13}$$

From equations (12) and (13) available:

$$F = mg + f_d = k_m \frac{\sin^2(\theta_0 + K_{p1}\Delta d / K_{p2})}{(d_0 + \Delta d + \Delta d_f)^2} \tag{14}$$

According formula(14) analysis, when the air gap $\Delta d$ is constant, adjusting $K_{p1}$ and $K_{p2}$ can adjust the levitation force F. Therefore, the levitation force F may be preset according to the amount of air gap variation $\Delta d$.

Take $\delta$ as the small displacement near the equilibrium position, and design the levitation force F as a function of the air gap. The design rules according to the different air gaps are as follows:

$$F = \begin{cases} F_1(d), d < d_0 - \delta \\ F_2(d), d_0 - \delta < d < d_0 + \delta \\ F_3(d), d > d_0 + \delta \end{cases} \tag{15}$$

The levitation force setting rules are shown in Figure 11.When the actual air gap $d<d0-\delta$，Suspended object has the tendency of attract to magnetic conductor, so anti-attract control should be done,levitation force is taken as $F_1(d)$.When $d<d_0+\delta$，The tendency of suspended object to fall,so adopt anti-fall control,levitation force is taken as $F_3(d)$.When $d_0-\delta<d<d_0+\delta$,To make the system more stable,$F_2(d)$ should be taken as the levitation force.

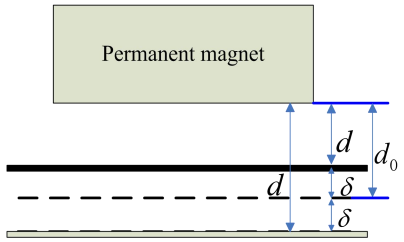


Fig. 11 Levitation force setting rules

According to the working principle of the disc permanent magnet, when the rotation angle $\theta$=90°, there is a maximum suspension force $F_{max}$.When the rotation angle $\theta$ is 0°,generating a minimum levitation force $F_{min}$ .As shown in Fig.12, when the suspended object fall to the maximum air gap, the angle of the permanent magnet is 90°,Generated upward force $f_1$ = F-*mg*. The permanent magnet is 0° when the suspension is attract to the minimum air gap，Generated downward force $f_2$ = mg.

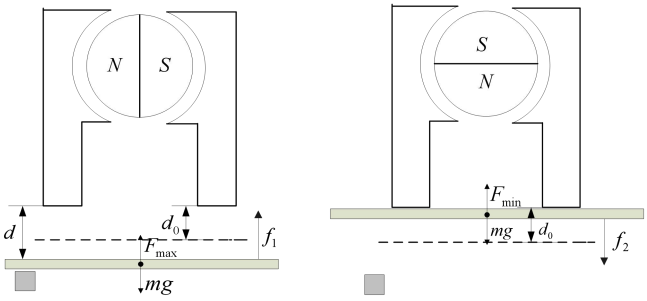


Fig. 12 System external force

According to the data in Table 1, it can be concluded that $F_{max}$=3.7N, $F_{min}$=0N, $f_1$=1.12N, $f_2$=2.6N. Combining the design rules of the levitation force F of Formula (14) and Formula (15),According to the set levitation force F, reverse derivation the ratio k of the control parameters $K_{P1}$ and $K_{P2}$. Then use numerical interpolation in the 2.5mm-6.5mm range, to obtain a complete control law *k*(*d*) of anti-fall-attract control. Figure 13 is a comparison of the levitation force of the PID control parameters k1 and anti-fall-attract control law *k*(*d*).

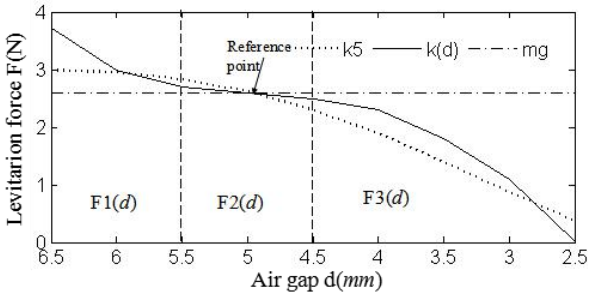


Fig. 13 Comparison of the levitation force of the PID control parameters $k_5$ and anti-fall-attract control law k(d)

As can be seen from the figure, Anti-fall anti-attract control reduces the difference between the levitation force F and the gravity mg near the equilibrium point, which improves the stability of the system;In the air gap *d*=6.5*mm* where the levitation force becomes larger, it can prevent falling;In the air gap *d*=2.5*mm* the levitation force F=0,It can prevent adsorption to the permanent magnet under gravity.

Figure 14 is a schematic diagram of anti-drop anti-fall anti attract control.

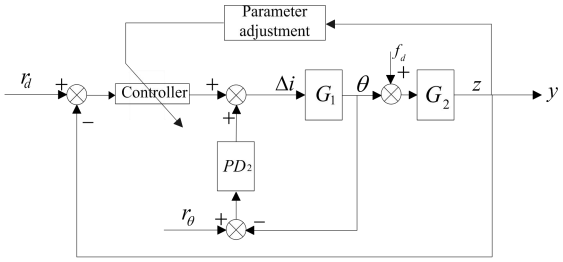


Fig. 14 Control schematic

The control quantity u(t) can be expressed as:

$$u(t) = k(d)\cdot z + Kd_1\dot{z} + Kp_2\Delta\theta + Kd_2\Delta\dot{\theta} \quad (16)$$

# 4 Simulation analysis and experimental verification

## 4.1 Simulation analysis

As shown in Fig.15,simulation results of the system for air gap *d*, permanent magnet rotation angle $\theta$, and current *i* are shown.When the suspended object is in a stable state, the external load increment of 0.26N is added to the suspended object at the time of 1s, 2s, 3s, 4s.Using anti-fall anti-attract controller and PID controller simulation contrast.

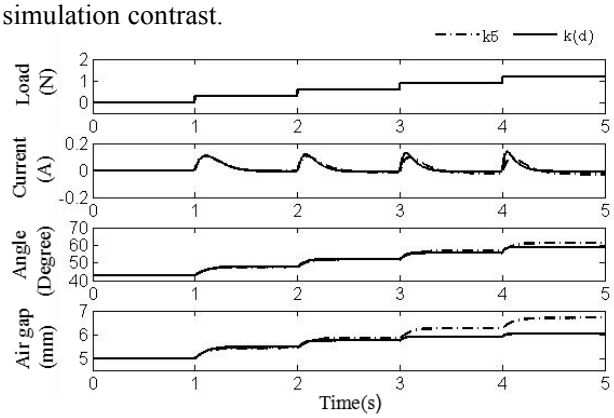


Fig. 15 System Simulation Analysis

As can be seen from Fig.15, when the external force gradually becomes larger, under the action of the anti-fall anti-attract controller, the air gap change amount of the suspended matter becomes smaller and smaller.When the load is cumulatively added to 1.04N, the air gap variation during the PID control is 2.8*mm*, and the air gap variation during the control of the anti-fall anti-attract control is 1.1*mm*.Air gap changes reduce 1.7mm.

## 4.2 Experiment analysis

As shown in Figure 16, Use force sensor to measure the resultant force of the system. The results are shown in Figure 17.

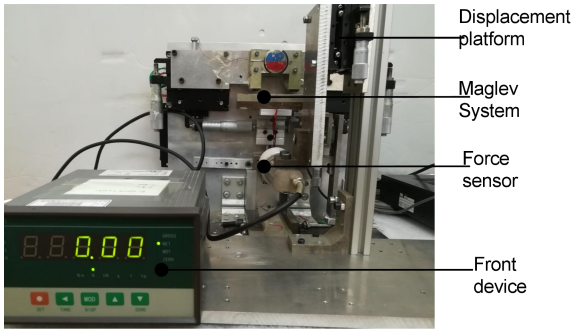


Fig. 16 Levitation force measurement experiment

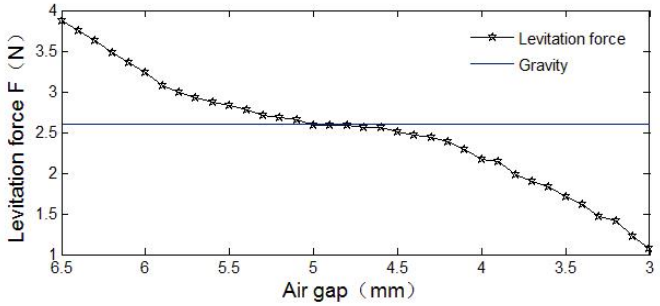


Fig. 17 Diagram of Maglev control experiment

In order to further verify the control effect of the controller, the control parameters are the same as those in the simulation analysis.After the system is stabilized, the same load is added, and the experimental results are shown in Fig. 18.

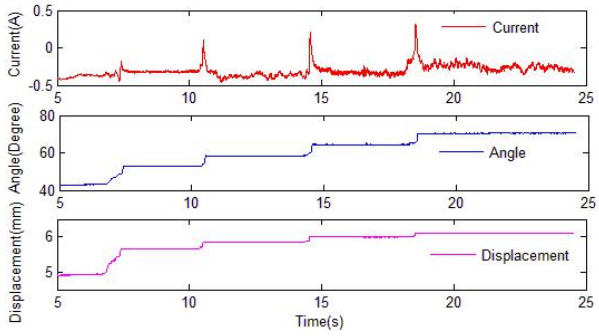


Fig. 18 Experimental verification

From the experimental data, it can be seen that with the increase of load, the change of suspension displacement becomes smaller and smaller, which plays an important role in mitigating the impact and preventing the fall.

# Conclusion

1)The results show that this method can effectively compensate for the uneven variation of the levitation force during the movement of the suspended substance. When the system is disturbed by a small external load, under the action of the real-time control system, the system can reach a new response time Stable state of suspension.

2)With the change of suspension air gap, the levitation force changes. When the air gap becomes larger, the levitation force becomes larger, which is much larger than the gravity of the suspended material, which can prevent the suspended material from falling down. When the floating air gap becomes smaller, the levitation force becomes smaller, Suspended solids gravity, to prevent suspended solids adsorption up.


## ACKNOWLEDGEMENTS

This research is supported by the following projects of Liaoning Province (No. LR2017036, No. 20170520177, No. 2015-47).


## REFERENCES


[1] LI Li-jun,FAN Yahong,YUAN Jun. Application of Magnetically Suspended Gimbaling Flywheel in Satellite Attitude Maneuver[J]. Journal of Mechanical Engineering,2015,51(16):206-212.

[2] ZHANG Gang,MENG Qing-tao,ZHONG Yong-yan,etal. Stable Levitation Performance Analysis of Five Degrees of Freedom All Permanent Magnetic Bearing System[J]. Journal of Mechanical Engineering,2015,51(5):56-63.

[3] WANG Keren,LUO Shihui,ZONG Ling-xiao. A dynamic simulation analysis of new maglev trains[J]. Journal of Vibration and Shock,2017,36(20):23-29.

[4] WAN Fukai,ZENG Pei,RU Weimin. Permanent Maglev Impeller Blood Pump and Analysis of Its Rotator Suspension[J]. Beijing Biomedical Engineering,2005,24(3):199-203.

[5] CHEN Guirong,LI Yungang,CHENG Hu. Application of NdFeB Permanent Magnet in Magnetic Levitation Technology[J].Chinese Rare Earths,2007,28(6):98-101.

[6] TIAN Lulin,YANG Xiaoping,LIYan,etal. Analytical Magnetic Force Model for Permanent Magnetic Guideway and Permanent Magnetic Bearings[J]. Journal of Tribology,2008,28(1):73-77.

[7] LI Qi-nan,CHEN Min,XU De-hong. Acceleration Feedback Control for Steel Plate Magnetic Suspension System[J].Proceedings of the CSEE ,2010,30(36):123-128.

[8] LIU Xu. Study On The Suspension Control Technology of The Magev Train[D]. National University of Defense Technology,2013:14-20.

[9] ZHANG Ying,CHEN Hui-xing,LI Yun-gang. Study on Protection Against Suspension Contact in Hybrid EMS Maglev Train[J].Ordnance Industry Automation,2009,28(1):59-61.

[10]CHEN Qiang,LI Xiao-long,LIU Shao-ke. Nonlinear PID Control for Levitation System of Maglev Train[J]. Electric Drive for Locmotives,2014(1):52-54.

[11] LIU Heng-kun,HAO A-ming,CHANG Wen-sen. Nonlinear PID Control of Magnetic Suspension Systems[J]. Control Engineering of China,2007,14(6):653-656.